Synthesis of urban CO_2 emission estimates from multiple methods from the Indianapolis Flux Project (INFLUX)

Jocelyn C. Turnbull[1,2,*], Anna Karion[3], Kenneth J. Davis[4], Thomas Lauvaux[4], Natasha L. Miles[4], Scott J. Richardson[4], Colm Sweeney[5], Kathryn McKain[2,5], Scott J. Lehman[6], Kevin R. Gurney[7], Risa Patarasuk[7], Jianming Liang[7], Paul B. Shepson[8], Alexie Heimburger[8], Rebecca Harvey[8], James Whetstone[3]

[1]GNS Science, Rafter Radiocarbon Laboratory, Lower Hutt, New Zealand
[2]CIRES, University of Colorado, Boulder, CO, USA
[3]NIST, Gaithersburg, MD, USA
[4]Pennsylvania State University, State College, PA, USA
[5]NOAA/ESRL, Boulder, CO, USA
[6]INSTAAR, University of Colorado, Boulder, CO, USA
[7]Arizona State University, Tempe, AZ, USA
[8]Purdue University, West Lafayette, IN, USA
*Rafter Radiocarbon Laboratory, GNS Science, 30 Gracefield Rd, Lower Hutt, New Zealand;
j.turnbull@gns.cri.nz

Abstract

Urban areas contribute approximately three-quarters of fossil fuel derived CO_2 emissions, and many cities have enacted emissions mitigation plans. Evaluation of the effectiveness of mitigation efforts will require measurement of both the emission rate and its change over space and time. The relative performance of different emission estimation methods is a critical requirement to support mitigation efforts. Here we compare results of CO_2 emissions estimation methods including an inventory-based method and two different top-down atmospheric measurement approaches implemented for the Indianapolis, Indiana, USA urban area in winter. By accounting for differences in spatial and temporal coverage, as well as trace gas species measured, we find agreement among the wintertime whole-city fossil fuel CO_2 emission rate estimates to within 7 %. This finding represents a major improvement over previous comparisons of urban-scale emissions, making urban CO_2 flux estimates from this study consistent with local and global emission mitigation strategy needs. The complementary application of multiple scientifically-driven emissions quantification methods enables and establishes this high level of confidence and demonstrates the strength of the joint implementation of rigorous inventory and atmospheric emissions monitoring approaches.

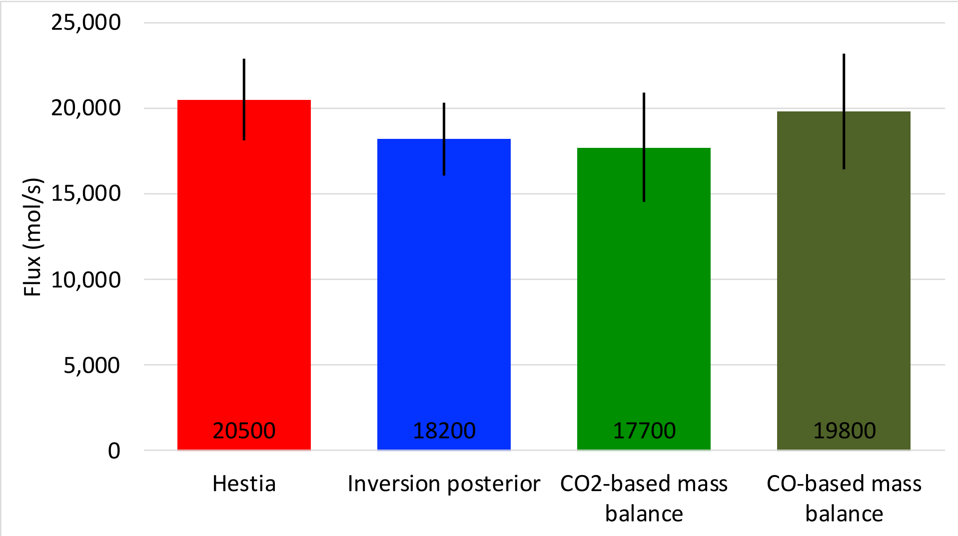
25,000
20,000
15,000
10,000
5,000
0
Flux (mol/s)
20500
18200
17700
19800
Hestia
Inversion posterior
CO2-based mass balance
CO-based mass balance

Introduction

Urban areas comprise only 3 % of Earth's surface area, but account for ~70 % of global fossil fuel derived carbon dioxide (CO_2ff) emissions [1]. Cities are leading the way in efforts to reduce emissions, with many cities having specific goals for emissions reductions (e.g. c40.org, globalcovenantofmayors.org). Under the Lima-Paris Action Agenda of the Paris Agreement, cities have a formalized role in mitigation strategies [2], and indeed many national mitigation objectives will be implemented by local governments and cities. Moreover, policy actions for low-carbon activities and carbon mitigation often provide additional benefits that are important to cities, such as reduced traffic congestion, improved air quality, noise reduction, reduced dependence on imported fuels and potentially improved quality of life and associated economic growth [3].

In order to evaluate the efficacy of low-carbon and greenhouse gas (GHG) strategies, cities will require continually updated knowledge of GHG emission rates. Ideally, emission information will have the precision and temporal resolution sufficient to evaluate emission trends through time, as well as information about the specific emission source sectors and spatial patterns of emissions within the urban area[4]. Two key questions are: what is the magnitude of whole-city CO_2 emissions; and what is the associated level of uncertainty? City-wide emission estimates have traditionally been obtained using inventory-based methodologies, often adopted from the international Intergovernmental Panel on Climate Change (IPCC) approach and downscaled to the urban scale [5-6]. However, a review of traditional urban inventories reveals a mixture of methods and data sources making it difficult to compare cities or assess accuracy or consistency over time[7-9], although efforts to standardize methodologies are underway[10-11]. Uncertainties in these city-scale emission estimates may be 50 to 100 % [12-13], insufficient to evaluate emission reduction policies. Under the Paris Agreement Nationally Determined Contributions, nations have committed to emission reductions of about 12 % by 2030 relative to extrapolation of current policy initiatives[14], and many cities propose to reduce their emissions by 30 - 50 % over the next 20 to 40 years, equating to 7.5 – 25% decreases per decade (e.g. c40.org; data.cdp.net). These goals suggest that the ability to evaluate urban emissions with an uncertainty of 10 % or less will be needed to provide meaningful assessments of progress.

A number of efforts have begun to evaluate urban emissions more rigorously using a variety of methods. For example, detailed inventory-based methodologies can provide high-resolution information on urban emission rates[12, 15], with emissions separated by source sectors and spatially and temporally distributed within a city and its surrounds. While these methods have the potential to revolutionize urban emissions information, they require detailed knowledge of all relevant emissions processes and their strengths and have uncertainties that are difficult to quantify.

Atmospheric mass balance methods have been used to evaluate urban CO_2 fluxes independent of inventory-based methods. Early work used an aircraft-based mass balance technique to evaluate CO_2 and CH_4 emissions from Indianapolis, and found a standard deviation of 80 % in whole-city CO_2 emission rate estimates for different days measured over a period of roughly one year[16]. A slightly different aircraft-based mass balance technique was used to estimate London's CO_2 emission rate, finding a range of about 100 % in their results[17]. These studies identified wind speed as the main source of uncertainty along with possible aliasing associated with low sampling frequency. More recent mass balance studies in Indianapolis have achieved improved standard deviation of 20 to 30 %

through better meteorological parameter determination[18-19]. Uncertainties in the mass balance method have primarily been evaluated by comparing flux estimates for multiple days with one another, using the reasonable assumption that day-to-day variability in the emission rate for individual weekday afternoons over a period of a few weeks is likely to be smaller than the variability induced by the mass balance methodology. Thus the comparison of multiple days provides an assessment of repeatability but not of systematic biases.

Another approach is to combine atmospheric ground or tower-based in-situ observations with atmospheric transport modelling. A comparison of simulated CO_2 mole fractions derived from a bottom-up inventory and atmospheric transport model with observed CO_2 mole fractions in the Salt Lake City region suggested that this methodology could detect changes in emissions of around 15 %[20]. Using similar methodologies along with more sophisticated inversion frameworks, several studies have estimated CO_2 emissions for Paris[21], London[22], Rotterdam[23], Boston[24], and Indianapolis[25]. In the Indianapolis inversion study, sensitivities to a range of assumptions embedded within the inversion method were assessed, but the overall uncertainty and potential biases of results were not quantified.

Indianapolis is one of the few urban areas where multiple emission assessment methods have been implemented, providing a unique opportunity to compare different methods directly. The Indianapolis Flux Experiment (INFLUX) aims to develop, assess, and minimize uncertainties of methods for quantifying greenhouse gas emissions at the urban scale, using the Indianapolis urban area (Figure 1) as a testbed[26]. INFLUX goals include determining whole-city emissions of CO_2 and methane, differentiating biogenic and anthropogenic CO_2 sources (including source sector allocation), reducing uncertainty in urban emission estimates and, ultimately, providing emission information at 1 km^2 spatial and weekly temporal resolution. Here we focus on the whole city CO_2 emission rate and compare three different approaches: a science-driven high-resolution urban inventory-based emission data product, an atmospheric transport model inversion based on in situ tower observations, and mass balance flux estimates from aircraft observations. We evaluate differences between the methods, particularly focusing on the use of discrete flask-based measurements to determine fossil fuel CO_2 separately from biogenic CO_2 contributions, and on the contribution of background CO_2 mole fractions to the urban flux estimates. Only winter-time emissions are considered, in order to minimize complications associated with biospheric CO_2 fluxes in this first attempt to compare differences between methods.

Whole city emission rate evaluation methods

Hestia data product

The Hestia high resolution inventory-based data product[15] provides anthropogenic CO_2 emission estimates for Indianapolis and the surrounding area (Figure 2). The Hestia approach has now also been implemented in Salt Lake City, Baltimore, and the Los Angeles Basin. It combines multiple data sources that represent a mix of emission-related content and include direct reporting of CO_2 fluxes, reporting of local air pollution (i.e. CO emission reporting), activity data (e.g. traffic counts, aircraft landing/takeoff statistics), fuel consumption statistics, and a variety of sociodemographic statistics. A series of datasets were also used to perform temporal and spatial distribution/downscaling for multiple scales and included data such as building footprints, roads and building occupancy schedules. It includes anthropogenic CO_2 emissions from eight sectors: onroad traffic, offroad vehicles (e.g. construction and farm equipment), railroads, airports, utilities (electricity generation), industry, commercial and residential. Only direct emissions occurring in the domain are considered. There is a small, known contribution of bio-ethanol that is included in gasoline sold in Indiana (10 %, Energy Independence and Security Act of 2007). Mobile emissions comprise 36 % of Hestia's total emissions, of which 75 % is gasoline combustion[15]. Therefore bio-ethanol contributes 3 % of the total Hestia CO_2 emissions and we scale Hestia down by this amount to obtain CO_2ff alone. We assign an initial uncertainty of 12 % to the whole-city Hestia flux, although this is somewhat based on expert judgement since uncertainty is quite difficult to evaluate for this methodology[25].

Atmospheric inversion

The atmospheric inversion[25] utilizes in situ CO_2 observations from 13 towers in and around Indianapolis (Figure 1). The inversion starts with the Hestia "prior" anthropogenic emissions and adjusts the emissions to give the best match with the tower observed CO_2 mole fractions resulting in a posterior flux map for the same domain as Hestia. The posterior flux is resolved spatially (1 x 1 km) and hourly but not by source sector. The analytical solution is calculated for five-day averaged estimates using a Bayesian inversion framework. Only observational data from the afternoon is used (1600 to 2200 UTC, 1100 to 1700 LST), when the model best simulates atmospheric transport. Given the typical transit time of air across Indianapolis of a few hours, the inversion is most sensitive to midday fluxes, is weakly sensitive to early morning fluxes and has very little sensitivity to evening and nighttime fluxes. Since the inversion utilizes CO_2 mole fraction observations, the inversion posterior flux represents the net CO_2 flux including all anthropogenic and biogenic fluxes. To isolate the CO_2 flux inside the domain, the background CO_2 mole fraction is defined by observations from one of the upwind towers (typically either Tower 1 or 9) and adjusted for fluxes that occur upwind of the upwind tower but inside the model domain. Uncertainty was estimated from the one-sigma scatter of 16 different applications of the inverse flux estimate[25]. This estimate does not include an explicit calculation of uncertainty in atmospheric transport, but earlier work suggests that the atmospheric model used here has modest random error (19° in wind direction and 0.8 m s^{-1} in wind speed) and small systematic errors (2° in wind direction and 0.1 ms-1) at this time of year[27]. While the spatial distribution of emissions is affected by these model errors, this has little effect on the aggregated flux over the entire domain[27]. Since the atmospheric inversion starts with the Hestia emission map as a prior, the inversion results are not entirely independent of the Hestia product. Full details of the atmospheric inversion are described elsewhere[23].

In the initial study [25], the inversion posterior resulted in 20% higher total emissions than Hestia for the period September 2012 – April 2013 (Table 1). The difference was likely due to that fact that the observational methods calculate total incremental CO_2 including both anthropogenic and biogenic fluxes, whereas the inventory-based product includes only anthropogenic sources[28]. This explanation is supported by studies demonstrating that although fossil fuel fluxes might be expected to dominate the overall CO_2 emission rate in urban areas, even in the dormant season biogenic CO_2 fluxes increase the total CO_2 flux by 10 - 20% in Indianapolis[28-29] and other cities show a similar pattern[30-32].

Aircraft Mass balance

High resolution in situ CO_2 measurements are made from an aircraft flying downwind of the urban area (varying by day depending on wind direction) at several different altitudes, typically between 12:00 – 16:00 LST (1700 – 2100 UTC). From these, a “curtain” of CO_2 mole fraction observations downwind of the city is developed. Concurrent measurements of wind speed and wind direction allow the CO_2 and CO (also CH_4) emission fluxes from the city to be determined[16, 18-19]. The emission rate is calculated relative to a background determined from the mole fractions measured in the edges of the downwind transects on the same day. Full details of the method and uncertainties can be found elsewhere[19]. Here we only consider the nine flights in November and early December 2014, when we expect that the CO_2 emission rate did not vary substantially from day to day[19] and to avoid the additional complication of strong photosynthetic drawdown in summer. Like the inversion, the aircraft mass balance method evaluates the net CO_2 flux including both anthropogenic and biogenic CO_2 emissions. The aircraft mass balance is independent of both Hestia and the inversion, except for the background correction that is later applied (see later section "Accounting for choice of CO_2 background"). The CO_2 and CO flux estimates use different mole fraction data but are linked through the use of the same wind observations. Investigation of the potential impacts of non-steady atmospheric conditions, and heterogeneous upwind boundary conditions may yield further improvements in the accuracy and precision of aircraft mass balance estimates.

Accounting for differences between methods

Evaluation of CO_2ff vs total CO_2 emissions

Hestia compiles data for anthropogenic CO_2 emissions (from fossil fuel CO_2 and bioethanol combustion). The atmospheric inversion and aircraft mass balance methods both estimate the net total urban enhancement in CO_2, which includes the influence of both anthropogenic and biogenic CO_2 fluxes. To resolve this incompatibility, we use flask measurements of $^{14}CO_2$ to determine the recently added CO_2ff[29], along with urban excess (enhancement over background) in CO_2 (CO_2xs) and in carbon monoxide (COxs) and derive empirical relationships between CO_2xs, CO_2ff and CO (Table 2).

Flasks collected in November and December from seven of the 13 towers between 2010 and 2016 (151 flasks) and during aircraft flights over and downwind of Indianapolis in November and December of 2010 to 2015 (40 flasks) are included in the analysis. Tower flask samples were collected only during westerly wind conditions so that Tower 1 was upwind of the city (Figure 1) and background was determined from the Tower one measurements. For the aircraft flights, background was defined by a flask measurement collected in the edges of downwind aircraft transects or upwind of the city on the same day. CO_2ff was calculated from the observed $\Delta^{14}CO_2$ and background $\Delta^{14}CO_2$ in the same flasks[29]. The CO_2:CO_2ff ratio was determined by regressing CO_2 against CO_2ff using an ordinary least squares bisector method (Table 2, Fig S1) and the CO:CO_2ff ratio was determined in a similar manner (Fig S1). In both cases, the aircraft dataset gives a slightly, but not significantly, higher ratio and reasons for this are discussed in the supplementary material.

We obtain a CO_2xs:CO_2ff ratio of 1.1 ± 0.1 ppm/ppm from the flask measurements for the months of November and December, implying that 10 ± 10 % of the CO_2xs is due to a local source other than CO_2ff. At a continental location such as Indianapolis, this can only be a net biogenic source that is greater than the background biogenic CO_2 fluxes. This is consistent with the known Indianapolis biogenic sources including human and pet respiration, biomass burning (home wood fires and a small power plant in Indianapolis that utilizes biomass[15]) and soil respiration. Together, these have been estimated to contribute 2,400 to 3,000 mol s^{-1} of biogenic CO_2 for Indianapolis in winter (13 - 16 % of the Hestia-derived CO_2ff emission rate)[28]. A similar calculation, but including flask measurements for the months September to April inclusive, gives a slightly higher ratio of 1.2 ± 0.1 ppm/ppm, and is consistent with the September to April biogenic CO_2 flux estimate from a previous study that estimated the wintertime urban biogenic flux, human and pet respiration and known biofuel CO_2 sources within the city[28]. Thus, we reduce the total CO_2 whole-city emission rate estimates from the atmospheric inversion and the mass balance by a factor of 1.1 ± 0.1 to obtain whole-city CO_2ff emission rate estimates from each of these methods (Table S2).

Samples are also measured for CO, which allows us to obtain a fourth, largely independent, CO_2ff flux estimate that avoids altogether the use of total CO_2 measurements and the associated biogenic CO_2 flux. Instead, in situ CO measurements from the aircraft flights are used in a mass balance calculation analogous to that for CO_2 to determine the whole-city CO emission rate of 108 ± 22 mol s^{-1} [19](Supp Table 2). We then scale whole city CO emission rate by the CO:CO_2ff ratio of 7 ± 2 ppb CO/ppm CO_2ff (Table 2; Fig S1) to determine a CO-based CO_2ff emission rate. Wintertime CO sources in Indianapolis are expected to be almost entirely from fossil fuel combustion, with about 1 % from biomass burning such as home fireplaces[29, 33-34], thus no attempt is made to correct for the biomass burning source.

Geographic region adjustment

The geographic area for which emissions are evaluated differs among the different methods. Hestia and the atmospheric inversion both evaluate fluxes for the same explicitly defined 87 x 87 km^2 domain that roughly comprises the nine counties that include and surround the Indianapolis metropolitan area (Figure 1). The aircraft mass balance evaluates fluxes for a (smaller) area that is less well defined and which will differ somewhat for each flight. To compare with the other methods, we define the aircraft footprint, or area of influence, as a box over the city (Figure 2)[35]. Determined from the location of the downwind flight path and drawing lines upwind the points on either side of the city where the urban emission plume is no longer distinguishable from the regional background CO_2 signal[19]. The aircraft footprint varies by flight (Table S2, Figure S2) and is 48 ± 6 % of the full Hestia 87 x 87 km^2 domain, determined from the mean and standard deviation of the fraction of the domain over the nine flights.

Time of day and time period of flux assessment

The Hestia CO_2 emission rate estimate reported in Table 1 is the mean flux over all hours of the day. The inversion posterior reports the mean emission rate for the entire diurnal cycle, but incorporates observational data only from the afternoon when the model best simulates atmospheric transport. Hence the inversion is least dependent on the Hestia prior in the midday hours. The aircraft mass balance measurements are always made during the afternoon and are therefore also most sensitive to the daytime fluxes. Thus, we extract only daytime (1600 to 2100 UTC, 11 am to 4 pm local time) emissions from Hestia and the atmospheric inversion so that all methods are comparing approximately the same time of day, and the time of day when the inversion is least dependent on the Hestia prior. The daytime mean emission rate estimates are ~ 20 % higher than the full diurnal estimates for both Hestia and the inversion (Table S2), with the largest difference occurring in the nighttime hours when traffic and commercial sources are quite low[15]. There is some variability associated with rush hour and the normal working hours, but choosing a different span of hours between 1200 to 2300 UTC does not significantly impact our results.

The aircraft flights were all conducted on weekdays, which Hestia predicts have a 13 % higher emission rate than the average across all days of the week, primarily driven by lower emissions on Sundays. In addition, factors such as ambient temperature (and therefore heating demand) and power plant loading result in day to day and seasonal emissions variability. The results previously reported[26] for Hestia and the inversion were both for the period of September 2012 to April 2013, whereas the aircraft estimates were from nine flights on weekdays in November and December 2014. Hestia has now been updated for all of 2014, and we therefore subsample Hestia for the same afternoons as the nine aircraft flights. Similarly, the atmospheric inversion has now been extended to November 2014 using the same methodology[25]. We use the atmospheric inversion results for the same seven afternoons as the aircraft flights in November 2014 and estimate the atmospheric inversion results for the two flights on December 1 and 3 2014 as the afternoon flux for the same day of the week, two weeks prior on November 17 and 19, respectively (avoiding the Thanksgiving holiday in the last week of November). Both the inversion posterior and Hestia results show that the mid-afternoon fluxes are quite consistent for each day of the week across the five weeks of November and the first week of December (±100 mol s^{-1} one sigma scatter across the five weeks) so this approximation is reasonable.

Accounting for choice of CO_2 background

A final factor that must be accounted for is that the Hestia inventory-based methodology sums all known anthropogenic fossil fuel combustion emissions within its domain. In contrast, to isolate the emissions occurring in the Indianapolis domain, the atmospheric methods remove (subtract) the incoming "background" CO_2 signal from the measurements within, or downwind of, the urban area to obtain the CO_2 excess (CO_2xs). In principle, the background CO_2 signal would be the CO_2 mole fraction that would have been measured at the observation site in the absence of the urban emissions. This is an unmeasurable quantity, so in practice, we define the background either as the CO_2 mole fraction at a tower that is immediately upwind of the urban area on a given day (atmospheric inversion) or by linearly interpolating the CO_2 mole fractions measured on the two edges of each downwind transect where the urban emission plume can no longer be discerned (mass balance). We also assume that the background CO_2 mole fraction is consistent spatially (i.e. across all upwind areas) and over the time it takes for air to transit over the city. This is a more reasonable assumption in our wintertime analysis period when the biosphere is dormant. During the growing season the biogenic CO_2 flux is large and varies both due to heterogeneity of land cover, the diurnal cycles of photosynthesis and respiration, and weather patterns.

In the case of the atmospheric inversion, the CO_2 mole fraction of air entering the model domain is subtracted from the observations before the inversion is performed, so that only the CO_2 emitted within the domain is considered in the inversion posterior. Ideally this background CO_2, or boundary condition, would be known for every point on the model domain boundaries. In practice, it is approximated from observations, larger scale model simulations, or some combination thereof. Urban mesoscale inversions including INFLUX have thus far primarily used upwind tower observations[20-21, 24-25]. For each day, the background CO_2 signal is determined from the instrumented tower that is upwind of the urban area. A further adjustment is applied to account for the modest CO_2 fluxes that occur within the model domain, but upwind of the tower chosen as background, such that the simulated footprint of the upwind tower on each day is convolved with the prior fluxes from Hestia to obtain a prediction of CO_2xs at the upwind tower relative to the upwind model domain boundary; this is subtracted from the upwind tower CO_2 mole fraction to determine the background expected at the model domain boundary[25]. The inversion posterior result therefore does not require further adjustment for its fossil fuel background fluxes before comparing to the inventory. This approach assumes that there are no differential influences in upwind versus downwind CO_2 that originate outside of the 87x87 km^2 inversion domain (e.g. a narrow fossil fuel CO_2 plume that influences the downwind measurements but is not captured at the upwind site).

In the case of the aircraft mass balance, the measurements from the edges of the downwind transects are used to determine the background CO_2 signal. The edges are defined as the point outside the city where the urban plume can no longer be detected (Figure 2). Yet Hestia predicts that the CO_2ff flux outside the aircraft footprint but inside the Hestia domain is non-zero due to modest emissions from roads and small towns (Figure 1). This can be expected to result in a small but significant increase in the edge CO_2 mole fraction relative to what would have been measured in the absence of those rural emissions (Figure 2). To account for this effect, we determine the mean flux in the rural area outside the aircraft footprint from Hestia, which varies slightly by flight and averages 1.5 ± 0.2 mol s^{-1} km^{-2} over all flights. We add this Hestia-determined flux per unit area to each gridbox within the aircraft footprint and sum to obtain a background-corrected aircraft mass balance flux (Table S2).

Results and discussion

The urban CO_2 emission rates for each method, as first reported in the original papers[15, 19, 25], range from 14,600 to 22,400 mol s^{-1} (Table 1). In aggregate, they have a one-sigma scatter of 21 % and the highest (inversion) and lowest (mass balance) differ by 42 %. Although an improvement over previous uncertainty estimates for urban emissions of 50 – 100 % from other studies[12-13], the initial INFLUX uncertainties as represented by differences between methods are nevertheless insufficient for detection of emissions trends on the order 10 % per decade.

Once the differences between methods are accounted for as described in this paper, the spread of values for the different methods of determining the whole city CO_2ff emission rate is 17,700 mol s^{-1} (CO_2-based mass balance) to 20,500 mol s^{-1} (Hestia), a difference of 15 % between the minimum and maximum estimates (Table 1, Figure 3). The impact of each adjustment on each method is given in Table S2. In summary, for Hestia the adjusted value is higher than the initial value because subsampling the (higher emission) afternoon period had a larger effect over the smaller footprint area. In contrast, the adjusted value is lower than the initial value for the inversion, where the different time period and the adjustment from total CO_2 to CO_2ff were more important. The adjusted mass balance value was reduced by the conversion from total CO_2 to CO_2ff but increased by the background correction. Overall, each of the adjustments (time period, time of day, day of week, geographic region, CO_2ff vs CO_2, background correction) altered the initial emission rate calculation for that method by -20 to +30 %, with no single adjustment dominating the others.

The four different realizations of the whole city CO_2ff emission rate from three largely independent methods give a weighted mean emission rate of 19,000 mol s^{-1}. The four methods all agree within their assigned uncertainties and the four mean values have a standard deviation of 1,300 mol s^{-1} (7 %) at one-sigma (Table 1, Figure 3). We separately calculate a standard error of 1,300 mol s^{-1} (7 %) from the four realizations, using the uncertainties assigned to each method. Comparison of the standard deviation and standard error can be used to evaluate the appropriateness of the uncertainties assigned to each individual method. When the uncertainties are too large (too small), the standard error will by larger (smaller) than the standard deviation. For our comparison, the consistency between the standard deviation and the standard error imply that the assigned uncertainties of 12 – 18 % (Table 1) for each method are appropriate. We note that the level of uncertainty achieved here requires iteration between top-down and inventory-based methods.

This study represents the first comprehensive, multiple-method assessment of urban CO_2ff emissions, and the agreement across these demonstrates for the first time CO_2ff emission uncertainty bounds informative for mitigation effort management. We conclude that the methodologies described here can, at least for Indianapolis, be applied collectively to provide emission rates with uncertainties of better than 10 % that will be useful within time frames appropriate to agreed international mitigation approaches/objectives. For example, the Indianapolis City Government aims to be carbon neutral by 2050[36]. Achieving half of that goal by emission reductions would require a 2 % yr^{-1} emission rate decrease. Given annual determination of the emission rate with 10 % uncertainty, this trend would be detectable with 95 % confidence in eight years. By increasing the frequency of the emission rate determinations to four times per year, the same trend could be detected with 95 % confidence after only five years, a common time period for reassessment of emissions.

The analysis presented here is for wintertime, when the biogenic CO_2 flux is small and consistently positive in Indianapolis, with little or no photosynthetic uptake. Relating the total CO_2 measurements used in the atmospheric methods to the fossil fuel CO_2 emission rate will be more challenging during times when the biosphere is more active with large and varying biogenic CO_2 fluxes both within and around the urban area. One path forward is to expand the use of the combined flask $^{14}CO_2$ and in situ CO measurements to evaluate the CO_2ff emission rate[30, 37-38]. Other ancillary anthropogenic trace gases may be worth investigating[39-40]. Improved control on the biogenic CO_2 fluxes inside and outside the city is an area of active research through both modelling[24, 31] and measurement that will likely yield significant improvements.

The greatly improved agreement between methods suggests that any of these methods could be employed alone to evaluate urban emissions, although the uncertainties and biases in each method could vary depending on the characteristics of any individual city[41]. The inventory-based data product offers detailed emission maps and process information, yet the large data-gathering effort required means it will be more practical in some cities than others. An atmospheric inversion based on long-term observations provides the opportunity to evaluate changes in emissions through time and has been shown to give robust results even with simpler prior flux estimates such as the ODIAC product[25, 42], but requires a long-term commitment to measurement infrastructure. The aircraft mass balance method could more quickly provide emission rate estimates for a suite of cities using a single instrumented aircraft, albeit with limited time resolution for each city. Importantly, use of any single method will continue to limit the ability to assess methodological bias and uncertainty.

Acknowledgements

This work has been funded by grants from the National Institute of Standards and Technology (NIST) with additional support from the National Oceanic and Atmospheric Administration Climate Program Office (NOAA-CPO). The flask-based trace gas and radiocarbon measurements were made possible by the ongoing hard work by NOAA/ESRL, University of Colorado INSTAAR and GNS Science staff.

References

1. Seto, K. C.; Dhakal, S.; Bigio, A.; Blanco, H.; D'elgado, G.; Dewar, D.; Huang, L.; Inaba, A.; Kansal, A.; Lwasa, S.; McMahon, J.; Müller, D.; Murakami, J.; Nagendra, H.; Ramaswami, A., Human settlements, infrastructure, and spatial planning. In *Climate Change 2014: Mitigation of Climate Change. Contribution of Working Group III to the Fifth Assessment Report of the Intergovernmental Panel on Climate Change*, Edenhofer, O., R. Pichs-Madruga, Y. Sokona, E. Farahani, S. Kadner, K. Seyboth, A. Adler, I. Baum, S. Brunner, P. Eickemeier, B. Kriemann, J. Savolainen, S. Schlömer, C. von Stechow, T. Zwickel and J.C. Minx, Ed. Cambridge University Press: Cambridge, United Kingdom and New York, NY, USA, 2014.
2. Ho, H.; Walsh, K. *The low carbon investment landscape in C40 cities: an analysis of the sustainable infrastructure projects currently in development across C40 cities* C40 Cities: New York, 2017.
3. Bai, X.; Dawson, R. J.; Ürge-Vorsatz, D.; Delgado, G. C.; Barau, A. S.; Dhakal, S.; Dodman, D.; Leonardsen, L.; Masson-Delmotte, V.; Roberts, D.; Schultz, S., Six research priorities for cities and climate change. *Nature* **2018,** *555*, 23-25.
4. Gurney, K. R.; Romero-Lankao, P.; Seto, K. C.; Hutyra, L.; Duren, R. M.; Kennedy, C. A.; Grimm, N. B.; Ehlringer, J. R.; Marcotullio, P.; Hughes, S.; Pincetl, S.; Chester, M. V.; Runfola, D. M.; Feddema, J. J.; Sperling, J., Tracking emissions on a human scale. *Nature* **2015,** *525*, 179-181.
5. Sovacool, B. K.; Brown, M. A., Twelve metropolitan carbon footprints: A preliminary comparative global assessment. *Energy Policy* **2010,** *38* (9), 4856-4869.
6. Hoornweg, D.; Sugar, L.; Trejos Gómez, C. L., Cities and greenhouse gas emissions: moving forward. *Environment and Urbanization* **2011,** *23* (1), 207-227.
7. Ibrahim, N.; Sugar, L.; Hoornweg, D.; Kennedy, C., Greenhouse gas emissions from cities: comparison of international inventory frameworks. *The International Journal of Justice and Sustainability* **2012,** *17* (2), 223-241.
8. Lombardi, M.; Laiola, E.; Tricase, C.; Rana, R., Assessing the urban carbon footprint: An overview. *Environmental Impact Assessment Review* **2017,** *66*, 43-52.
9. Ramaswami, A.; Chavez, A., What metrics best reflect the energy and carbon intensity of cities? Insights from theory and modeling of 20 US cities. *Environmental Research Letters* **2013,** *8* (3).
10. Fong, W. K.; Sotos, M.; Doust, M.; Schultz, S.; Marques, A.; Deng-Beck, C. *Global Protocol for Community-Scale Greenhouse Gas Emission Inventories*; 2014.
11. ICLEI, International local government GHG emissions analysis protocol (IEAP). **2009**.
12. Gately, C. K.; Hutyra, L. R., Large Uncertainties in Urban-Scale Carbon Emissions. *Journal of geophysical Research Atmospheres* **2017**.
13. Pacala, S. W.; Breidenich, C.; Brewer, P. G.; Fung, I. Y.; Gunson, M. R.; Heddle, G.; Law, B. E.; Marland, G.; Paustian, K.; Prather, M.; Randerson, J. T.; Tans, P. P.; Wofsy, S. C., *Verifying greenhouse gas emissions: Methods to support international climate agreements; Committee on Methods for Estimating Greenhouse Gas Emissions; National Research Council*. National Academies Press: Washington, DC, 2010.
14. UNEP *The Emissions Gap Report 2017 A UN Enviornment Synthesis Report*; Nairobi, 2017.
15. Gurney, K. R.; Razlivanov, I.; Song, Y.; Zhou, Y.; Benes, B.; Abdul-Massih, M., Quantification of Fossil Fuel CO_2 Emissions on the Building/Street Scale for a Large U.S. City. *Environmental Science & Technology* **2012,** *46* (21), 12194-12202.

16. Mays, K. L.; Shepson, P. B.; Stirm, B. H.; Karion, A.; Sweeney, C.; Gurney, K. R., Aircraft-based measurements of the carbon footprint of Indianapolis. *Environmental Science and Technology* **2009,** *43*, 7316-7823.

17. Font, A.; Grimmond, C. S.; Kotthaus, S.; Morgui, J. A.; Stockdale, C.; O'Connor, E.; Priestman, M.; Barratt, B., Daytime CO2 urban surface fluxes from airborne measurements, eddy-covariance observations and emissions inventory in Greater London. *Environnetal Pollution* **2015,** *196*, 98-106.

18. Cambaliza, M. O.; Shepson, P. B.; Caulton, D.; Stirm, B.; Samarov, D.; Gurney, K. R.; Turnbull, J.; Davis, K. J.; Possolo, A.; Karion, A.; Sweeney, C.; Moser, B.; Hendricks, A.; Lauvaux, T.; Mays, K.; Whetstone, J.; Huang, J.; Razlivanov, I.; Miles, N. L.; Richardson, S. J., Assessment of uncertainties of an aircraft-based mass-balance approach for quantifying urban greenhouse gas emissions. *Atmospheric Chemistry and Physics Discussions* **2013,** *13* (11), 29895-29945.

19. Heimburger, A. M.; Harvey, R. M.; Shepson, P. B.; Stirm, B. H.; Gore, C.; Turnbull, J. C.; Cambaliza, M. O. L.; Salmon, O. E.; Kerlo, A.-E.; Lavoie, T. N.; Davis, K. J.; Lauvaux, T.; Karion, A.; Sweeney, C.; Brewer, W. A.; Hardesty, R. M.; Gurney, K. R., Assessing the optimized precision of the aircraft mass balance method for measurement of urban greenhouse gas emission rates through averaging. *Elementa: Science of the Anthropocene* **2017,** *5* (26).

20. McKain, K.; Wofsy, S. C.; Nehrkorn, T.; Eluszkiewicz, J.; Ehleringer, J. R.; Stephens, B. B., Assessment of ground-based atmospheric observations for verification of greenhouse gas emissions from an urban region. *Proceedings of the National Academy of Sciences* **2012,** *109* (22), 8423-8428.

21. Staufer, J.; Broquet, G.; Bréon, F.-M.; Puygrenier, V.; Chevallier, F.; Xueref-Rémy, I.; Dieudonné, E.; Lopez, M.; Schmidt, M.; Ramonet, M.; Perrussel, O.; Lac, C.; Wu, L.; Ciais, P., The first 1-year-long estimate of the Paris region fossil fuel CO₂ emissions based on atmospheric inversion. *Atmospheric Chemistry and Physics* **2016,** *16* (22), 14703-14726.

22. Boon, A.; Broquet, G.; Clifford, D. J.; Chevallier, F.; Butterfield, D. M.; Pison, I.; Ramonet, M.; Paris, J.-D.; Ciais, P., Analysis of the potential of near-ground measurements of CO₂ and CH₄ in London, UK, for the monitoring of city-scale emissions using an atmospheric transport model. *Atmospheric Chemistry and Physics* **2016,** *16* (11), 6735-6756.

23. Super, I.; Denier van der Gon, H. A. C.; van der Molen, M. K.; Sterk, H. A. M.; Hensen, A.; Peters, W., A multi-model approach to monitor emissions of CO₂ and CO from an urban–industrial complex. *Atmospheric Chemistry and Physics* **2017,** *17* (21), 13297-13316.

24. Sargent, M.; Barrera, Y.; Nehrkorn, T.; Hutyra, L. R.; Gately, C. K.; Jones, T.; McKain, K.; Sweeney, C.; Hegarty, J.; Hardiman, B.; Wofsy, S. C., Anthropogenic and biogenic CO2 fluxes in the Boston urban region. *Proceedings of the National Academy of Sciences of the United States of America* **2018,** *115* (29), 7491-7496.

25. Lauvaux, T.; Deng, A.; Miles, N. L.; Richardson, S.; Gurney, K. R.; Patarasuk, R.; Razlivanov, I.; Juang, J.; Gaudet, B.; Sarmiento, D.; Wu, K.; Davis, K. J.; Oda, T.; Shepson, P. B.; Cambaliza, M. O.; Karion, A.; Sweeney, C.; Turnbull, J. C., High resolution atmospheric inversion of urban CO_2 emissions during the dormant season of the Indianapolis Flux Experiment (INFLUX). *Journal of geophysical Research Atmospheres* **2016,** *121*.

26. Davis, K. J.; Deng, A.; Lauvaux, T.; Miles, N. L.; Richardson, S. J.; Sarmiento, D. P.; Gurney, K. R.; Hardesty, R. M.; Bonin, T. A.; Brewer, W. A.; Lamb, B. K.; Shepson, P. B.; Harvey, R. M.; Cambaliza, M. O.; Sweeney, C.; Turnbull, J. C.; Whetstone, J.; Karion, A., The Indianapolis Flux Experiment (INFLUX): A test-bed for developing urban greenhouse gas emission measurements. *Elem Sci Anth* **2017,** *5* (0), 21.

27. Deng, A.; Lauvaux, T.; Davis, K. J.; Gaudet, B.; Miles, N. L.; Richardson, S. J.; Wu, K.; Sarmiento, D.; Hardesty, M.; Bonin, T. A.; Brewer, A.; Gurney, K. R., Toward reduced transport errors in a high resolution urban CO2 inversion system. *Elementa* **2017,** *5*, 20.

28. Gurney, K. R.; Liang, J.; Patarasuk, R.; O'Keeffe, D.; Huang, J.; Hutchins, M.; Lauvaux, T.; Turnbull, J. C.; Shepson, P. B., Reconciling the differences between a bottom-up and inverse-estimated FFCO2 emissions estimate in a large US urban area. *Elementa: Science of the Anthropocene* **2017,** *5* (44).

29. Turnbull, J. C.; Sweeney, C.; Karion, A.; Newberger, T.; Lehman, S. J.; Tans, P. P.; Davis, K. J.; Lauvaux, T.; Miles, N. L.; Richardson, S. J.; Cambaliza, M. O.; Shepson, P. B.; Gurney, K.; Patarasuk, R.; Razlivanov, I., Toward quantification and source sector identification of fossil fuel CO2 emissions from an urban area: Results from the INFLUX experiment. *Journal of Geophysical Research: Atmospheres* **2015**.

30. Djuricin, S.; Pataki, D. E.; Xu, X., A comparison of tracer methods for quantifying CO_2 sources in an urban region. *Journal of Geophysical Research* **2010,** *115* (D11).

31. Hardiman, B. S.; Wang, J. A.; Hutyra, L. R.; Gately, C. K.; Getson, J. M.; Friedl, M. A., Accounting for urban biogenic fluxes in regional carbon budgets. *The Science of the total environment* **2017,** *592*, 366-372.

32. Pataki, D. E., Seasonal cycle of carbon dioxide and its isotopic composition in an urban atmosphere: Anthropogenic and biogenic effects. *Journal of Geophysical Research* **2003,** *108* (D23).

33. USEPA *2011 National Emissions Inventory, version 1 Technical Support Document*; US Environmental Protection Agency, Office of Air Quality Planning and Standards, Air Quality Assessment Division: Research Triangle Park, North Carolina, 2013.

34. Vimont, I. J.; Turnbull, J. C.; Petrenko, V. V.; Place, P. F.; Karion, A.; Miles, N. L.; Richardson, S. J.; Gurney, K. R.; Patarasuk, R.; Sweeney, C.; Vaughn, B. H.; White, J. W. C., Carbon monoxide isotopic measurements in Indianapolis constrain urban source isotopic signatures and support mobile fossil fuel emissions as the dominant wintertime CO source. *Elementa: Science of the Anthropocene* **2017,** *5* (63).

35. Zavala-Araiza, D.; Lyon, D. R.; Alvarez, R. A.; Davis, K. J.; Harriss, R.; Herndon, S. C.; Karion, A.; Kort, E. A.; Lamb, B. K.; Lan, X.; Marchese, A. J.; Pacala, S. W.; Robinson, A. L.; Shepson, P. B.; Sweeney, C.; Talbot, R.; Townsend-Small, A.; Yacovitch, T. I.; Zimmerle, D. J.; Hamburg, S. P., Reconciling divergent estimates of oil and gas methane emissions. *Proceedings of the National Academy of Sciences of the United States of America* **2015,** *112* (51), 15597-602.

36. City of Indianapolis *Thrive Indianapolis Draft*; City of Indianapolis: Indianapolis, USA, 2018.

37. Levin, I.; Karstens, U. T. E., Inferring high-resolution fossil fuel CO_2 records at continental sites from combined $^{14}CO_2$ and CO observations. *Tellus B* **2007,** *59* (2), 245-250.

38. Turnbull, J. C.; Karion, A.; Fischer, M. L.; Faloona, I.; Guilderson, T.; Lehman, S. J.; Miller, B. R.; Miller, J. B.; Montzka, S.; Sherwood, T.; Saripalli, S.; Sweeney, C.; Tans, P. P., Assessment of fossil fuel carbon dioxide and other anthropogenic trace gas emissions from

airborne measurements over Sacramento, California in spring 2009. *Atmospheric Chemistry and Physics* **2011,** *11* (2), 705-721.

39. Coakley, K. J.; Miller, J. B.; Montzka, S. A.; Sweeney, C.; Miller, B. R., Surrogate gas prediction model as a proxy for Δ14C-based measurements of fossil fuel−CO2. *Journal of Geophysical Research: Atmospheres* **2016**.

40. Nathan, B.; Lauvaux, T.; Turnbull, J. C.; Gurney, K. R., Investigations into the use of multi-species measurements for source apportionment of the Indianapolis fossil fuel CO2 signal. *Elementa: Science of the Anthropocene* **2018,** *6* (21).

41. Hutyra, L. R.; Duren, R.; Gurney, K. R.; Grimm, N.; Kort, E. A.; Larson, E.; Shrestha, G., Urbanization and the carbon cycle: Current capabilities and research outlook from the natural sciences perspective. *Earth's Future* **2014,** *2* (10), 473-495.

42. Oda, T.; Maksyutov, S.; Andres, R. J., The Open-source Data Inventory for Anthropogenic CO₂, version 2016 (ODIAC2016): a global monthly fossil fuel CO₂ gridded emissions data product for tracer transport simulations and surface flux inversions. *Earth System Science Data* **2018,** *10* (1), 87-107.

583 **Tables**

584

585 Table 1. Methodologies and results for each CO_2 emission rate determination and the weighted mean and standard error of the four different methods. Initial CO_2 emission rates are the values and one sigma uncertainties reported in previous publications[15, 19, 25-26]. Adjusted CO_2ff emission rates are the values determined with the adjustments described in the text and representing the CO_2ff emission rate for nine days in November to December 2014, 11 to 16 LST, for the region representing the aircraft footprints, and the mass balance corrected for background. Uncertainties are based on the one sigma scatter of results for each of the nine flights. See supplementary material for individual flight values.

Method	**Includes…**	**Domain**	**Time of day**	**Time period**	**Initial CO_2 (mol/s)**	**Adjusted CO_2ff (mol/s)**
Hestia inventory-based	Fossil CO_2 + bioethanol	9 counties	All	Sep 2012 – Apr 2013	18,300 ± 2,200	20,500 ± 2,400
Inversion/ tower CO_2	Total CO_2	9 counties	All	Sep 2012 – Apr 2013	22,400 ± 500	18,200 ± 2,100
CO_2-based mass balance	Total CO_2	Aircraft footprint	Mid-afternoon	Nov – Dec 2014	14,600 ± 3,300	17,700 ± 3,200
CO-based mass balance	Fossil CO_2	Aircraft footprint	Mid-afternoon	Nov – Dec 2014	NA	19,800 ± 3,400
Weighted mean	**Fossil CO_2**	**Aircraft footprint**	**Mid-afternoon**	**Nov – Dec 2014**		**19,000 ± 1,300**

593

Table 2.Emission ratios for CO_2xs:CO_2ff and COxs:CO_2ff determined from flask samples collected from towers and aircraft from 2010 to 2016. Ratios and their one sigma uncertainty are determined from the correlation between CO_2ff and CO_2xs or COxs, using ordinary least squares bisector regression (Table S1; Figure S1).

	CO_2xs:CO_2ff **(ppm/ppm)** (n, r^2)	**COxs:CO_2ff** **(ppb/ppm)** (n, r^2)
All Nov – Dec	1.1 ± 0.1 (186, 0.8)	7 ± 2 (191, 0.6)
Towers Nov - Dec	1.1 ± 0.1 (151, 0.8)	7 ± 2 (151, 0.6)
Aircraft Nov - Dec	1.2 ± 0.1 (35, 0.9)	9 ± 2 (40, 0.7)
All Jan - Oct	NA	8 ± 1 (788, 0.5)

Figures

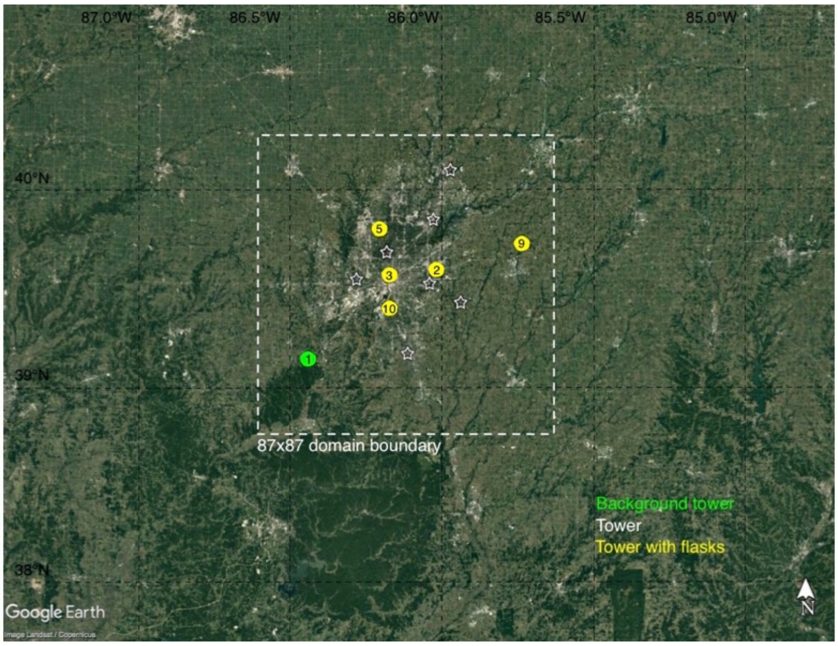

Figure 1. Map of Indianapolis region showing Hestia/inversion domain and the sampling towers.

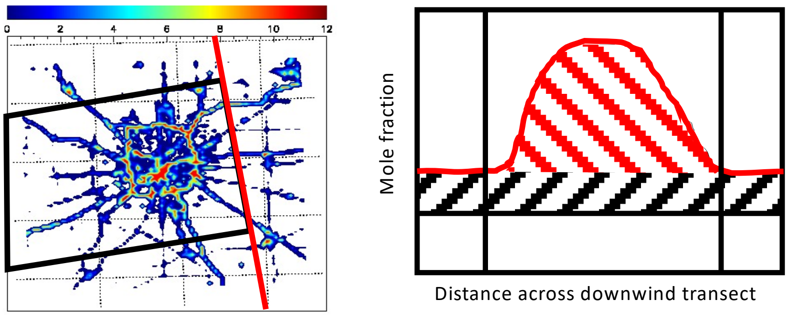

Figure 2. Left: Example of how the footprint area is determined for an aircraft mass-balance transect measurement, defined by the box enclosed by the black and red lines. For context, the footprint area is overlaid on the Hestia spatial distribution of emissions. Right: Schematic of CO_2 measurements for a single downwind transect. The solid red line indicates the downwind flight path where the CO_2 and CO measurements are made and used to determine the mass balance emission rate from the urban area. The edges of the urban plume are defined as the point where the urban CO_2 plume is not distinguishable, indicated by the vertical black lines in the right panel. To determine the footprint, lines are projected upwind from the edge points in the direction of the wind to the upwind edge of the Hestia domain as shown by the black box in the left panel. The effect of rural CO_2ff emissions is also shown in the right panel. If the CO_2ff flux in the rural area is zero, then the urban CO_2ff flux is defined by the red hatched area under the red curve. However, in the case that rural CO_2ff emissions are small but non-zero, the CO_2 mole fraction may not appear to vary in the edges but will still be elevated relative to what it would have been in the absence of those rural emissions, shown as the black hatched area. Thus, when rural emissions occur upwind of the edges of the downwind aircraft transect, the aircraft mass balance method will underestimate total urban emissions.

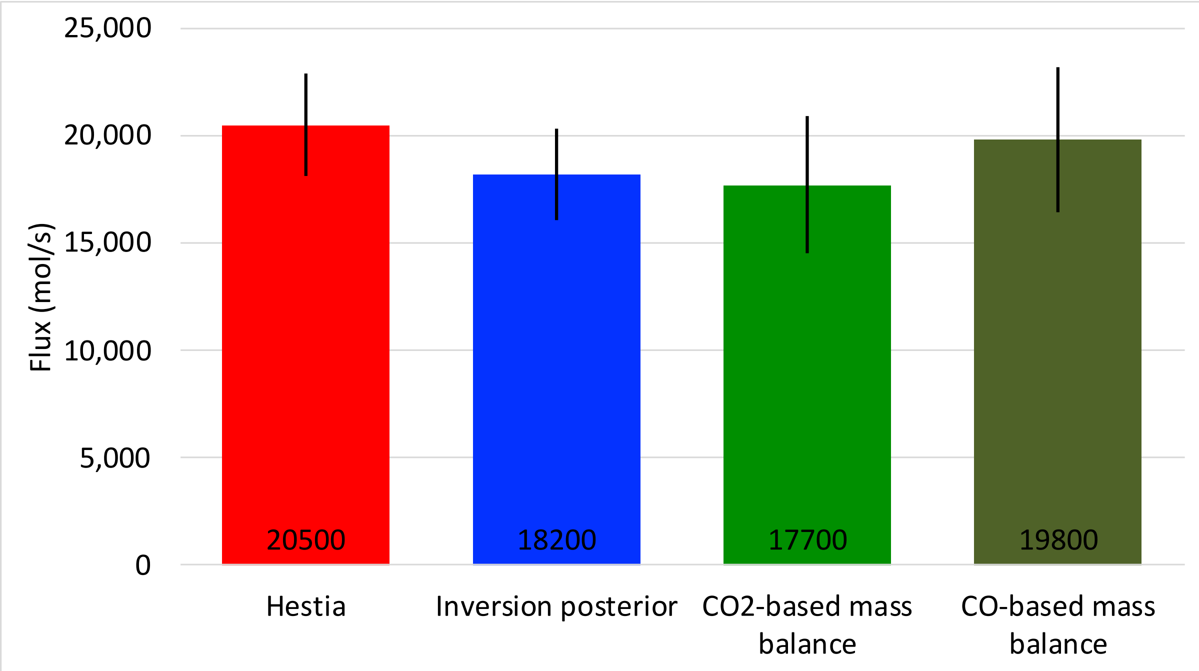

Figure 3. Adjusted CO_2ff emission rates. Values were determined with the adjustments described in the text and representing the CO_2ff emission rate for nine days in November to December 2014, midday hours only, for the region representing the aircraft footprints, and the mass balance corrected for background. Error bars are the one sigma scatter of the results for each of nine flights.

Supplementary Material

Supplementary Table 1.

Emission ratios for individual towers, aircraft and different time periods. The ratios determined for only November and December 2014 are not significantly different than those determined for all years 2010 – 2016, although the smaller dataset for the single year results in a larger uncertainty for COxs:CO_2ff. Defining “winter” as the months of September – April inclusive, as was used in previous INFLUX publications [1-2] results in a slightly higher CO_2xs:CO_2ff ratio and a somewhat weaker correlation. This is likely due to stronger biogenic CO_2 fluxes in the fall and spring months than in the colder, lower daylight hour months. There is no difference in the COxs:CO_2ff ratio for the longer winter period and larger dataset.

COxs:CO_2ff varies substantially between towers, and the aircraft result is slightly higher than the tower average. It is likely that this is related to sampling biases. The 151 November – December tower samples are from five different towers (supplementary material), and CO:CO_2ff ratio varies by tower, with the highest ratio (10 ± 2 ppb/ppm) observed at Tower two and the lowest at Tower ten (2 ± 1 ppb/ppm). This is consistent with Tower two being most influenced by traffic (with high CO:CO_2ff emission ratio) and Tower ten being strongly influenced by power plant emissions with low CO:CO_2ff emission ratio. Although five tower locations are not sufficient to perfectly observe the entire urban emissions, the mix of sites might be expected to give a reasonable approximation of overall emissions. In each aircraft flight, the limited number of flasks are deliberately collected in the urban plume, but outside the obvious (higher CO_2) power plant plume. Since the power plant has a very low

$CO:CO_2ff$ emission ratio[3], this can be expected to bias the aircraft samples to a higher $CO:CO_2ff$ ratio. Note that the aircraft in situ CO_2 and CO measurements are taken during the entire flight, including the power plant plume, so this applies only to the flask determinations. For $CO:CO_2ff$, there is no significant difference between winter and summer ratios (8 ± 1 for all 788 flasks), although other evidence[4] suggests that $CO:CO_2ff$ should be slightly higher in summer due to production of CO from volatile organic compounds.

	Slope $CO_2xs:CO_2ff$ (ppm/ppm) (n, r^2)	**Slope $COxs:CO_2ff$ (ppb/ppm)** (n, r^2)
All Nov – Dec	1.1 ± 0.1 (186, 0.8)	7 ± 2 (191, 0.6)
Towers Nov - Dec	1.1 ± 0.1 (151, 0.8)	7 ± 2 (151, 0.6)
Tower 2 Nov - Dec	1.1 ± 0.1 (37, 0.7)	10 ± 2 (37, 0.8)
Tower 3 Nov - Dec	1.1 ± 0.1 (34, 0.9)	5 ± 2 (34, 0.5)
Tower 5 Nov - Dec	1.1 ± 0.1 (29, 0.6)	8 ± 2 (29, 0.7)
Tower 9 Nov - Dec	1.2 ± 0.1 (33, 0.6)	6 ± 1 (33, 0.5)
Tower 10 Nov - Dec	1.1 ± 0.1 (9, 0.8)	2 ± 1 (9, 0.7)
Aircraft Nov - Dec	1.2 ± 0.1 (35, 0.9)	9 ± 2 (40, 0.7)
All Nov – Dec 2014 only	1.1 ± 0.1 (46, 0.8)	6 ± 3 (51, 0.5)
All Nov - Apr	1.2 ± 0.1 (472, 0.7)	7 ± 1 (476, 0.5)
All Sep - Apr	1.2 ± 0.1 (648, 0.6)	7 ± 1 (652, 0.5)
All Jan - Oct	NA	8 ± 1 (788, 0.5)
Towers Jan - Oct	NA	8 ± 1 (699, 0.5)
Aircraft Jan - Oct	NA	8 ± 1 (89, 0.5)

Supplementary Table 2.

Emission rates and other calculated values for each of the nine aircraft flights. The fraction of 87x87 km Hestia domain that is inside the aircraft footprint is given as % area in footprint (maps of the footprints are given in Supplementary Figure 2. The Initial CO_2 and CO_2 emission rates are given for the aircraft, along with CO_2ff calculated using emission ratios CO_2xs:CO_2ff of 1.1 ± 0.1 ppm/ppm and COxs:CO_2ff of 7 ± 2 ppb/ppm. Background corrected aircraft emission rates add the background correction for mass balance determined from Hestia, which is calculated by adding the CO_2 flux rate in the edges (outside the aircraft footprint) to every 1x1 km gridbox inside the aircraft footprint and summing across all gridboxes (see main text for explanation). Hestia 2014 uses the 1 km resolution 87x87 km gridded Hestia product for 2014. The CO_2 emission rate for the footprint is determined by subsampling for the aircraft footprint for that flight day, and averaging across the hours 1600 to 2100 UTC. CO_2ff emission rate in footprint is determined by scaling the CO_2 emission rate down by 3.5% to remove the bioethanol component. The CO_2 flux rate in the footprint and in edges are the mean flux rate in mol/s/km^2 for all gridboxes inside or outside the footprint, respectively. The fraction of the total emissions in the domain during that time that occur in the aircraft footprint is given as % emissions in footprint. The atmospheric inversion is reported at 1 km resolution on the same 87x87 km grid, and is sampled in the same manner as Hestia. The CO_2ff emission rates used in the comparison in the main text are shown in bold.

	Date	Nov. 13	Nov. 14	Nov. 17	Nov. 19	Nov. 20	Nov. 21	Nov. 25	Dec. 1	Dec. 3	**average**	**stdev**	**stdev (%)**
Aircraft mass balance	% area in footprint	50	48	52	40	49	56	52	39	50	**48**	**6**	**11%**
	CO_2 emission rate (mol/s)	13600	11700	19500	20200	13800	14000	14600	14000	10200	**14600**	**3300**	**23%**
	CO emission rate (mol/s)	111	119	139	96	111	101	129	100	62	**108**	**22**	**20%**
	CO_2ff emission rate from CO_2 (mol/s)	12364	10636	17727	18364	12545	12727	13273	12727	9273	**13300**	**3000**	**23%**
	CO_2ff from CO_2 bkgd corrected (mol/s)	**16489**	**15686**	**22765**	**23087**	**15661**	**17983**	**17720**	**16181**	**13625**	**17700**	**3200**	**18%**
	CO_2ff emission rate from CO (mol/s)	15857	17000	19857	13714	15857	14429	18429	14286	8857	**15400**	**3200**	**21%**
	CO_2ff from CO bkgd corrected (mol/s)	**19982**	**22050**	**24895**	**18437**	**18973**	**19684**	**22876**	**17739**	**13209**	**19800**	**3400**	**17%**
Hestia 2014	CO_2 emission rate in footprint (mol/s)	21400	21400	21100	21500	20200	18900	22600	19800	24300	**21200**	**1600**	**8%**
	CO_2ff emission rate in footprint (mol/s)	**20656**	**20656**	**20367**	**20753**	**19498**	**18243**	**21815**	**19112**	**23456**	**20500**	**1500**	**7%**
	CO_2 flux rate in footprint (mol/s/km^2)	5.7	5.9	5.4	7.0	5.4	4.4	5.7	6.8	6.4	**5.9**	**0.8**	**0.1**
	CO_2 flux rate in edges	1.1	1.4	1.3	1.6	0.8	1.2	1.1	1.2	1.2	**1.2**	**0.2**	**0.2**
	Bkgd correction for mass balance	4125	5050	5038	4723	3115	5256	4448	3454	4352	**4400**	**700**	**16%**
	% emissions in footprint	84	80	82	75	86	82	85	78	85	**82**	**4**	**5%**
Atmos-pheric inversion	CO_2 emission rate in footprint	21700	18900	21800	18000	20300	18700	20900	20800	19000	**20000**	**1400**	**7%**
	CO_2ff emission rate in footprint	**19727**	**17182**	**19818**	**16364**	**18455**	**17000**	**19000**	**18909**	**17273**	**18200**	**1300**	**7%**
	CO_2 flux rate in footprint	5.8	5.2	5.6	5.9	5.4	4.4	5.3	7.1	5.1	**5.5**	**0.7**	**13%**
	CO_2 flux rate in edges	1.3	1.3	1.2	1.1	1.3	0.9	1.2	1.2	1.0	**1.2**	**0.2**	**13%**
	% emissions in footprint	81	79	83	79	81	87	82	79	84	**82**	**3**	**3%**

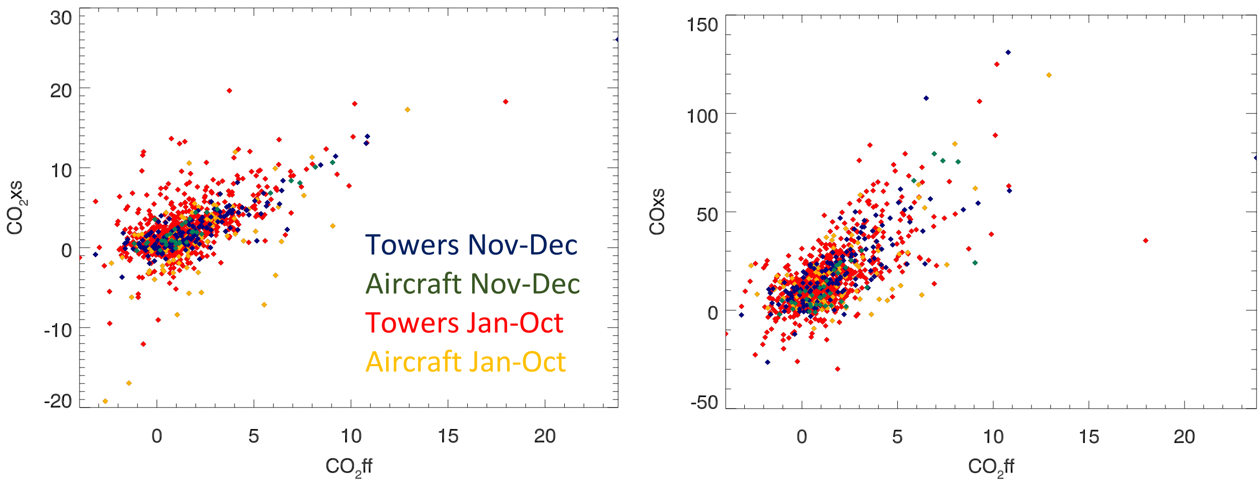

Supplementary Figure 1. Flask measurements of CO_2ff vs CO_2xs (left) and COxs (right) used to determine the ratios CO_2xs:CO_2ff and COxs:CO_2ff. Units are ppm for CO_2ff and CO_2xs and ppb for COxs. Ratios were determined using an ordinary least squares bisector method[3, 5].

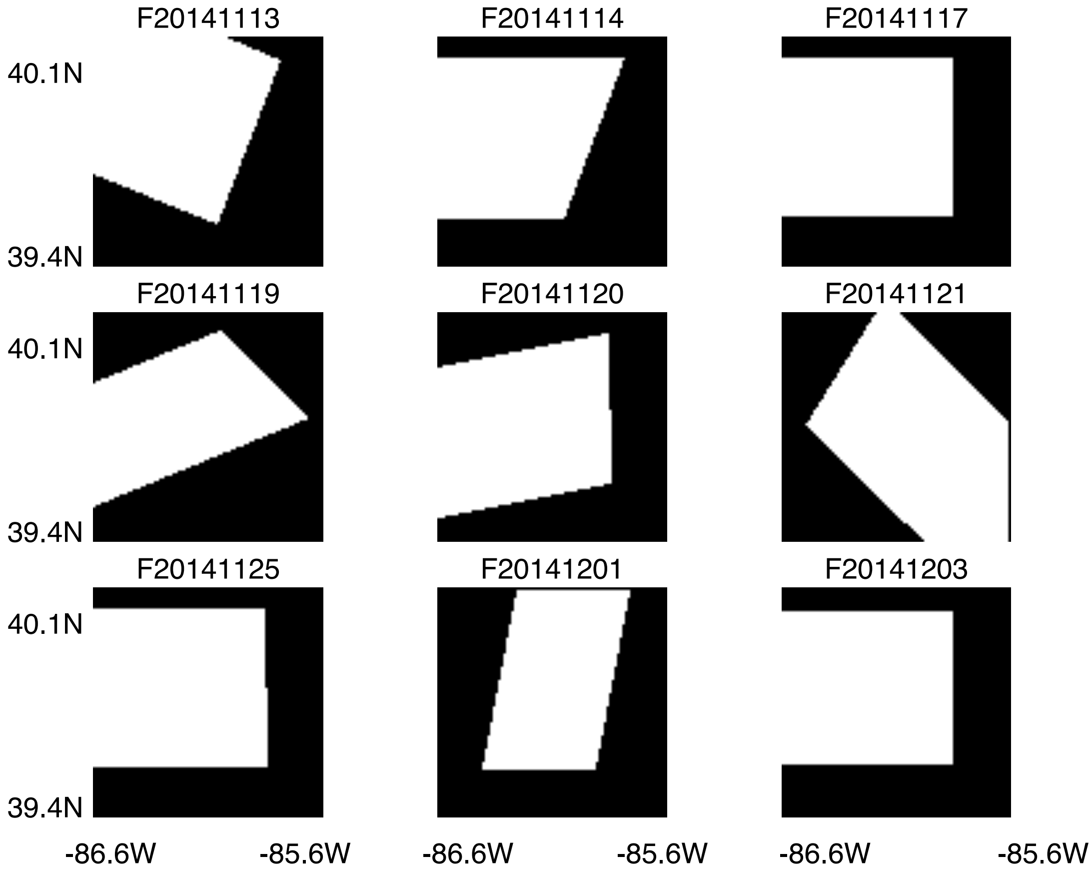

Supplementary Figure 2. Footprints for each of the nine flights. Flight names are listed as Fyyyymmdd. White area is the aircraft footprint and the black area is the area inside the domain but outside the aircraft footprint.

Supplementary References

1. Lauvaux, T.; Deng, A.; Miles, N. L.; Richardson, S.; Gurney, K. R.; Patarasuk, R.; Razlivanov, I.; Juang, J.; Gaudet, B.; Sarmiento, D.; Wu, K.; Davis, K. J.; Oda, T.; Shepson, P. B.; Cambaliza, M. O.; Karion, A.; Sweeney, C.; Turnbull, J. C., High resolution atmospheric inversion of urban CO_2 emissions during the dormant season of the Indianapolis Flux Experiment (INFLUX). *Journal of geophysical Research Atmospheres* **2016,** *121*.
2. Gurney, K. R.; Liang, J.; Patarasuk, R.; O'Keeffe, D.; Huang, J.; Hutchins, M.; Lauvaux, T.; Turnbull, J. C.; Shepson, P. B., Reconciling the differences between a bottom-up and inverse-estimated FFCO2 emissions estimate in a large US urban area. *Elementa: Science of the Anthropocene* **2017,** *5* (44).
3. Turnbull, J. C.; Sweeney, C.; Karion, A.; Newberger, T.; Lehman, S. J.; Tans, P. P.; Davis, K. J.; Lauvaux, T.; Miles, N. L.; Richardson, S. J.; Cambaliza, M. O.; Shepson, P. B.; Gurney, K.; Patarasuk, R.; Razlivanov, I., Toward quantification and source sector identification of fossil fuel CO2 emissions from an urban area: Results from the INFLUX experiment. *Journal of Geophysical Research: Atmospheres* **2015**.
4. Vimont, I. J.; Turnbull, J. C.; Petrenko, V. V.; Place, P. F.; Karion, A.; Miles, N. L.; Richardson, S. J.; Gurney, K. R.; Patarasuk, R.; Sweeney, C.; Vaughn, B. H.; White, J. W. C., Carbon monoxide isotopic measurements in Indianapolis constrain urban source isotopic signatures and support mobile fossil fuel emissions as the dominant wintertime CO source. *Elementa: Science of the Anthropocene* **2017,** *5* (63).
5. Carroll, R. J.; Ruppert, D.; Stefanski, L. A.; Crainiceanu, C. M., *Measurement Error in Nonlinear Models: A Modern Perspective*. Second ed.; CRC Press: United States, 2006; p 488.